

# Stability of $\alpha$ -Tocopherol in Freeze-Dried Sugar–Protein–Oil Emulsion Solids as Affected by Water Plasticization and Sugar Crystallization

Yankun Zhou and Yrjö H. Roos\*

Food Technology, School of Food and Nutritional Sciences, University College Cork, Cork, Ireland

**ABSTRACT:** Water plasticization of sugar–protein encapsulants may cause structural changes and decrease the stability of encapsulated compounds during storage. The retention of  $\alpha$ -tocopherol in freeze-dried lactose–milk protein–oil, lactose–soy protein–oil, trehalose–milk protein–oil, and trehalose–soy protein–oil systems at various water activities ( $a_w$ ) and in the presence of sugar crystallization was studied. Water sorption was determined gravimetrically. Glass transition and sugar crystallization were studied using differential scanning calorimetry and the retention of  $\alpha$ -tocopherol spectrophotometrically. The loss of  $\alpha$ -tocopherol followed lipid oxidation, but the greatest stability was found at 0  $a_w$ , presumably because of  $\alpha$ -tocopherol immobilization at interfaces and consequent reduction in antioxidant activity. A considerable loss of  $\alpha$ -tocopherol coincided with sugar crystallization. The results showed that glassy matrices may protect encapsulated  $\alpha$ -tocopherol; however, its role as an antioxidant at increasing  $a_w$  accelerated its loss. Sugar crystallization excluded the oil-containing  $\alpha$ -tocopherol from the protecting matrices and exposed it to surroundings, which decreased the stability of  $\alpha$ -tocopherol.

**KEYWORDS:** Encapsulation,  $\alpha$ -tocopherol, carbohydrate–protein, water activity, crystallization

## ■ INTRODUCTION

Vitamin E contributes to many biological functions, including enzymatic activities, gene expression activity, neurological function, and antioxidant activity.<sup>1</sup>  $\alpha$ -Tocopherol is the main vitamin E compound, with antioxidant activity that inhibits the formation and decomposition of hydroperoxides,<sup>2</sup> although it may become pro-oxidative at elevated concentrations.<sup>3,4</sup> Losses of  $\alpha$ -tocopherol in food systems could result from (i) degradation, which was affected by exposures to oxygen, light, and high temperatures,<sup>5,6</sup> as well as from (ii) its consumption as an antioxidant reactant in the presence of lipids, i.e., accelerated degradation during lipid oxidation.<sup>7–9</sup> Freeze-drying entraps and encapsulates sensitive compounds into a dry wall material, which may also enhance stability of bioactive components.<sup>10,11</sup> Encapsulation of the hydrophobic  $\alpha$ -tocopherol requires (i) breakdown of the lipid phase into small droplets by emulsification and dispersion of these droplets into the continuous aqueous phase, (ii) freezing to immobilize and encapsulate the lipid droplets in freeze-concentrated solutes, and (iii) stabilization of the system by sublimation of the ice.<sup>10,12</sup> Sugars are effective encapsulating agents because they form amorphous glassy solids that restrict the movement of entrapped and encapsulated compounds.<sup>10,11,13–17</sup> The glass formation occurs in freezing, and the stability of freeze-dried solid structures accounted for their glassy state. Plasticization resulting in glass transition of freeze-dried materials affects numerous changes in the storage of dried solids, e.g., crystallization of sugars.<sup>10,11,18</sup> Dehydrated sugar–protein mixtures showed delayed crystallization of component sugars<sup>19</sup> and showed reduced changes in solid structures. This suggested carbohydrate–protein systems as potential encapsulants. Proteins may also act as emulsifiers,<sup>20</sup> and the emulsification properties of proteins are important in the stabilization of hydrophobic nutrient delivery systems.

Widicus and others<sup>6</sup> reported first-order kinetics of degradation of  $\alpha$ -tocopherol in freeze-dried model systems containing no fat. The degradation rate of  $\alpha$ -tocopherol increased with increasing water activity ( $a_w$ ), and it was diffusion-dependent. Widicus and Kirk<sup>8</sup> found that, in freeze-dried model systems containing fat,  $\alpha$ -tocopherol degraded more rapidly than in systems containing no fat and followed the progression of lipid oxidation. In fat-containing systems, water affected the stability of  $\alpha$ -tocopherol through protecting lipids against oxidation by (i) hydrogen bonding to the hydroperoxides and (ii) hydration of metal catalysts, which made them less effective as a result of changes in their coordination sphere<sup>21</sup> up to 0.5  $a_w$ . At higher  $a_w$ , the rate of lipid oxidation increased with increasing  $a_w$ , because of the mobilization of catalysts and exposure of lipids to an increased number of catalysts (especially in swelling systems). However, the effects of physical changes, e.g., glass transition and crystallization of matrices, as a result of water sorption on the stability of  $\alpha$ -tocopherol have not been studied intensively. Especially at 0  $a_w$ , when lipid oxidation is rapid, the consumption of antioxidants may be assumed to be the most rapid. However, because of the polar paradox that hydrophobic antioxidants, e.g.,  $\alpha$ -tocopherol, are more active in emulsions than in oils,<sup>22,23</sup> we would expect  $\alpha$ -tocopherol to show less antioxidant activity in anhydrous systems, i.e., systems containing no water (similar to bulk oil systems).

The objectives of the present study were to encapsulate and stabilize emulsified oil droplets containing  $\alpha$ -tocopherol in amorphous carbohydrate–protein matrices by freezing and

Received: April 17, 2012

Revised: July 12, 2012

Accepted: July 13, 2012

Published: July 13, 2012

freeze-drying. The physicochemical properties (water sorption, glass transition, and crystallization) of the matrices and the stability of  $\alpha$ -tocopherol in these matrices, as affected by water activity and physical changes, were determined.

## MATERIALS AND METHODS

**Materials.**  $\alpha$ -Lactose monohydrate (Sigma-Aldrich, St. Louis, MO), trehalose dihydrate (Cargill, Inc., Minneapolis, MN), milk protein isolate (MPI; Kerry Ingredients, Listowel, Co., Kerry, Ireland), and soy protein isolate (SPI; PRO-FAM891, Archer Daniels Midland, Decatur, IL) were used as encapsulating matrices. Olive oil (OO; Extra Virgin Olive Oil, Don Carlos, Hacienda Don Carlos, purchased from the local market) was used as a lipid carrier for the hydrophobic  $\alpha$ -tocopherol (Sigma-Aldrich, St. Louis, MO). Reagents used for extraction of  $\alpha$ -tocopherol, including ascorbic acid, potassium hydroxide (KOH), methanol, butylated hydroxytoluene (BHT), *n*-hexane, and anhydrous sodium sulfate ( $\text{Na}_2\text{SO}_4$ ), were all purchased from Sigma-Aldrich (St. Louis, MO). Ethanol (Ethanol 100), which was also used for extraction of  $\alpha$ -tocopherol, was purchased from Carbon Group (Carbon Group, Ringaskiddy, Co., Cork, Ireland).

**Preparation of Emulsions and the Freeze-Dried Materials.** Lactose–MPI (3:1), lactose–SPI (3:1), trehalose–MPI (3:1), and trehalose–SPI (3:1) suspensions were prepared [250 g, 20% (w/w) of solids] using distilled water. All materials were allowed to hydrate at 45 °C for at least 3 h, with an assumption of sufficient hydration of materials. The suspensions were reweighed, and the amount of water equivalent to the amount of evaporated water was added. The suspensions were left to cool to room temperature ( $24 \pm 1$  °C).  $\alpha$ -Tocopherol (5%, w/w) was mixed with olive oil, which naturally contains a smaller amount of  $\alpha$ -tocopherol than other oils,<sup>24</sup> under stirring at room temperature. The olive oil with  $\alpha$ -tocopherol (25 g) was mixed into the carbohydrate–protein suspensions (250 g), pre-homogenized using Ultra-Turrax (T25 Digital, Staufen, Germany) at 10 000 rpm for 30 s, and immediately homogenized at room temperature (APV-1000 high-pressure homogenizer, Wilmington, MA) at 24 MPa (two stages: 20 and 4 MPa) for 3 cycles.

Freshly prepared emulsions [275 g, 9.1% (w/w) oil phase] were transferred using an adjustable-volume pipet (Pipetman P5000, Gilson, Inc., Middleton, WI) into glass vials (clear glass ND18, 10 mL, VWR, U.K.) (5 mL per vial), frozen at  $-35$  °C ( $T_g' < T < T_m$ )<sup>19</sup> for 24 h, and subsequently transferred to a  $-80$  °C freezer for 5 h to avoid ice melting during transfer to a freeze-dryer (Lyovac GT2, STERIS, Hürth, Germany). Samples in glass vials with semi-closed rubber septa were freeze-dried for  $\geq 72$  h at  $<0.1$  mbar ( $T < -40$  °C). All vials at completion of freeze-drying were hermetically closed inside the freeze-dryer using the rubber septa prior to breaking the vacuum with ambient air. The freeze-dried lactose–MPI–OO (3:1:2), lactose–SPI–OO (3:1:2), trehalose–MPI–OO (3:1:2), and trehalose–SPI–OO (3:1:2) systems were theoretically composed of two parts of nonfat solids and one part of lipid, and  $\alpha$ -tocopherol accounted for 1.67% (w/w) of the total solids.

**Characterization of the Nonfat Solids: Water Sorption and Sorption Isotherms.** Triplicate samples of each freeze-dried emulsion in open vials were equilibrated up to 5 days at room temperature (in general,  $24 \pm 1$  °C) in evacuated desiccators over various saturated salt solutions, LiCl,  $\text{CH}_3\text{COOK}$ ,  $\text{MgCl}_2$ , and  $\text{K}_2\text{CO}_3$ , giving respective water activities ( $a_w$ ) of 0.11, 0.23, 0.33, and 0.44 at equilibrium.<sup>25</sup> The samples were weighed at 0, 3, 6, 9, 12, 24, 48, 72, 96, and 120 h. A gradual decrease of sorbed water indicated time-dependent lactose or trehalose crystallization. This was monitored during storage over saturated solutions of  $\text{Mg}(\text{NO}_3)_2$ ,  $\text{NaNO}_2$ , and  $\text{NaCl}$ , giving respective  $a_w$  of 0.54, 0.65, and 0.76 at equilibrium.<sup>25</sup> The vials with samples were weighed every 1 h up to 6 h, at 8, 10, 12, 24, 48, 72, 96, and 120 h. The water activity of the saturated salt solutions was confirmed using an Aqua Lab 4TE instrument (Decagon Devices, Inc., Pullman, WA). The water content of each material was measured gravimetrically as a function of time, and the mean weight of triplicate samples was calculated.<sup>26</sup>

The Guggenheim–Anderson–de Boer (GAB) equation was used to model water sorption.<sup>27</sup> The GAB isotherm parameters,  $m_m$  (monolayer value) and  $K$ , were obtained by plotting  $a_w$  against  $a_w/m$  and from a second-order polynomial regression over the  $a_w$  range from 0.11 to 0.44.

**Characterization of the Nonfat Solids: Glass Transition and Crystallization.** The onset,  $T_g$  (onset), and endset,  $T_g$  (endset), temperatures of glass transition and the instant crystallization temperature,  $T_{ic}$ , were measured using differential scanning calorimetry (DSC; Mettler Toledo 821e with liquid  $\text{N}_2$  cooling, Switzerland). The thermograms were analyzed using STAR thermal analysis software, version 6.0 (Mettler Toledo, Switzerland), as reported by Roos and Karel.<sup>28</sup> The freeze-dried materials were powdered using a spatula in glass vials. To determine the  $T_g$  (onset) and  $T_{ic}$ , 10–15 mg of the powdered freeze-dried materials were prepared in open DSC pans and equilibrated over  $\text{P}_2\text{O}_5$  and saturated salt solutions to  $a_w$  of 0–0.44 at room temperature. After equilibration, the pans were hermetically sealed and the samples were analyzed (Table 2) according to the report by Zhou and Roos.<sup>19</sup> Triplicate samples were analyzed for each material.

**Oil Droplet Size Distribution.** The droplet size distribution of emulsions was analyzed by laser diffraction (Malvern Mastersizer S, Malvern Instruments, Ltd., Malvern, U.K.) according to O'Regan and Mulvihill.<sup>29</sup> Fresh emulsions were analyzed within 1 h after preparation. Frozen emulsions after 24 h of storage at  $-35$  °C were thawed (room temperature for 1 h) and analyzed. Freeze-dried materials were reconstituted to the original weight, gently mixed, and analyzed. The droplet size ( $\mu\text{m}$ ) was reported as the volume-weight mean diameter,  $D[4, 3]$ , and the volume median diameter,  $D[v, 0.5]$ .

**Spectrophotometry of  $\alpha$ -Tocopherol.** The  $\alpha$ -tocopherol content was measured spectrophotometrically. The freeze-dried materials before and after storage were reconstituted to the original weight and vortexed for 30 s at high speed for mixing. Aliquots of 1 mL of the reconstituted emulsions were transferred into test tubes (20 mL) and destabilized by ethanol (3 mL). Ascorbic acid solution [5% (w/v), freshly made, 2 mL] was added to the mixtures to prevent oxidation in the liquids. Separation of  $\alpha$ -tocopherol (unsaponified fraction) from the oil (saponified fraction) was achieved by adding saturated KOH–methanol (1 mL) into the mixes and vortexing for 15 s, followed by holding at 45 °C in a water bath for 30 min. After cooling to room temperature,  $\alpha$ -tocopherol was extracted 3 times with *n*-hexane [with 0.1% (w/v) BHT, 2 mL], which was added into the mixes followed by vortexing for 30 s to extract  $\alpha$ -tocopherol. The mixes were left to stand for 10 min for the separation of the organic layer containing  $\alpha$ -tocopherol on the top and the water layer on the bottom. The organic layer was removed carefully using a glass Pasteur pipet (9 in., Corning, Inc., Corning, NY) into a glass vial containing anhydrous  $\text{Na}_2\text{SO}_4$  powder (about 0.5 g), which absorbed possible residual water (modified from the report by Cornacchia and Roos<sup>30</sup>). After 1:10 dilution with *n*-hexane (with BHT), the extracts were transferred into cuvettes (semi-micro, low-form, UV grade, Kartell, Italy), and the absorbance was measured at 297.7 nm using a spectrophotometer (Varian Cary 300, Bio UV–vis spectrophotometer, Agilent Technologies, Santa Clara, CA). This wavelength was found to correspond to the maximum absorbance of  $\alpha$ -tocopherol in *n*-hexane (with BHT) over the spectrum of wavelengths from 200 to 400 nm.<sup>31</sup> A standard curve was obtained by measuring absorbance of  $\alpha$ -tocopherol in *n*-hexane (with BHT) at various concentrations (0–125  $\mu\text{g}/\text{mL}$ ). The amount of  $\alpha$ -tocopherol in the olive oil was measured to adjust the actual amount of added  $\alpha$ -tocopherol, but this was, however, undetectable.

**Storage of the Freeze-Dried Materials and Stability of  $\alpha$ -Tocopherol.** To study the stability of  $\alpha$ -tocopherol in different encapsulants, the freeze-dried materials in closed vials were stored in an incubator at 60 °C for 40 days. The  $\alpha$ -tocopherol content was measured at intervals during storage. To study the effect of water activity and structural changes on the stability of  $\alpha$ -tocopherol, the freeze-dried materials in open vials were equilibrated for 5 days at room temperature ( $24 \pm 1$  °C) in evacuated desiccators over  $\text{P}_2\text{O}_5$  and various saturated salt solutions [ $\text{LiCl}$ ,  $\text{CH}_3\text{COOK}$ ,  $\text{MgCl}_2$ ,  $\text{K}_2\text{CO}_3$ ,

Mg(NO<sub>3</sub>)<sub>2</sub>, NaNO<sub>2</sub>, and NaCl], giving respective water activities ( $a_w$ ) of 0, 0.11, 0.23, 0.33, 0.44, 0.54, 0.65, and 0.76 at equilibrium, according to the water sorption results. The sample vials were closed manually with septa, sealed with parafilm, and then transferred into the incubator at 60 °C for 10 days. Because of the high porosity of the freeze-dried materials, the total volume of the glass vials (10 mL) was considered as the headspace volume during storage. The  $\alpha$ -tocopherol content was measured after (i) equilibration and (ii) incubation, and the ratio [content after incubation/content after equilibration]  $\times$  100 was calculated as percent retention.

**Statistics.** All measurements carried out in this study were performed in triplicate. The mean values of triplicate samples  $\pm$  1 standard deviation (SD) are reported as results for water sorption, glass transition and crystallization, and the stability study.

## RESULTS AND DISCUSSION

**Water Sorption and Sorption Isotherms.** Water sorption of freeze-dried lactose–MPI–OO, lactose–SPI–OO, trehalose–MPI–OO, and trehalose–SPI–OO systems over various  $a_w$  conditions as a function of time was plotted, as shown in Figure 1. The final water contents are given in Table

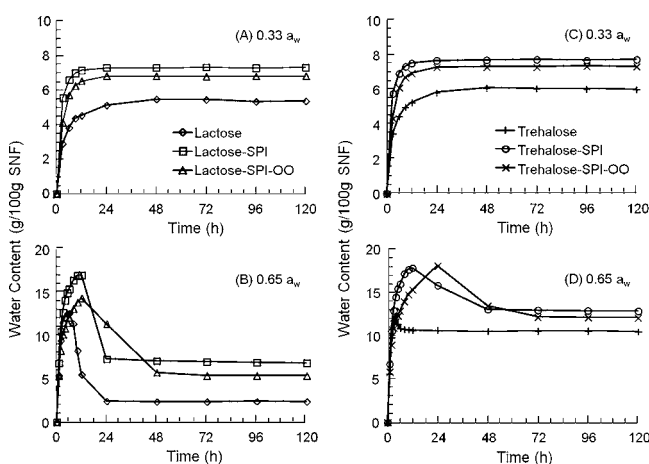


**Figure 1.** Water sorption [g/100 g of solid nonfat (SNF)] of freeze-dried lactose,<sup>19</sup> trehalose,<sup>19</sup> lactose–SPI (3:1),<sup>19</sup> trehalose–SPI (3:1),<sup>19</sup> lactose–SPI–OO (3:1:2), and trehalose–SPI–OO (3:1:2) systems at (A and C) 0.33  $a_w$  and (B and D) 0.65  $a_w$  at room temperature ( $24 \pm 1$  °C). The loss of water at 0.65  $a_w$  indicated sugar crystallization.

1. At low water activities up to 0.44  $a_w$ , sugar–protein systems showed the most rapid water sorption and the highest amounts of sorbed water, followed by sugar–protein–oil systems (panels A and C of Figure 1). Less water sorption in sugar–protein–oil systems compared to sugar–protein systems was possibly because of hydrophobic interactions between proteins and oils at the interface. This decreased the quantity of proteins in the sugar–protein-rich continuous phase.

Sugar crystallization was found at 0.54  $a_w$  and above for lactose and trehalose.<sup>19</sup> Delayed sugar crystallization occurred in sugar–protein and sugar–protein–oil systems as a result of interference with the mobility of lactose and trehalose molecules and possible interactions between sugars and proteins (panels B and D of Figure 1), e.g., by hydrogen bonding between sugars and proteins. A limited amount of hydrogen bonding between sugars and proteins, above which sugars and proteins exist as free components without interaction, has been reported, although the components were not necessarily completely immiscible, i.e., phase-separated but forming a homogeneous bulk.<sup>32</sup> Our earlier studies showed that at 3:1 ratio of sugars and proteins existed as phase-separated, largely immiscible glass formers,<sup>19,33</sup> which excluded major molecular interaction effects on sugar crystallization. At 0.65  $a_w$ , lactose crystallization was found after 6, 12, and 12 h for lactose, lactose–SPI, and lactose–SPI–OO systems, respectively. It appeared that lactose crystallization responsible for changes in sorbed water contents in the lactose–SPI–OO system (Figure 1B) proceeded more slowly at a lower water content than in the lactose–SPI system. Trehalose crystallization was found after 4, 12, and 24 h in trehalose, trehalose–protein, and trehalose–protein–oil systems, respectively (Figure 1D). Trehalose crystallization was less rapid in the sugar–protein–oil systems than in the sugar–protein systems. We assume that the dispersed oil phases with protein interfaces disturbed the continuous hydrophilic sugar–protein phase and hindered the movement of sugar molecules to form crystals. The molecular assemblies of the components occur in emulsification prior to freezing (protein–oil) and as a result of freeze concentration (protein–sugar). The protein molecules are likely to become covered by sugar molecules during freezing, and this structure can be retained to the freeze-dried systems. Diffusion of the sugar molecules at the molecular surfaces of proteins and the hydrophobic environment of oil droplets can reduce their nucleation and crystal growth rates.

The GAB model was fitted to the water sorption data. Sugar–protein systems at the low experimental  $a_w$  range showed the sigmoid sorption isotherms and highest water sorption, followed closely by sugar–protein–oil systems and then pure sugar systems (Figure 2). The lower amount of sorbed water in the nonfat solids of systems containing oil at each  $a_w$  condition could be due to the hydrophobic interactions between protein and oil, which decreased the amount of protein in the sugar–protein phases and their hydrogen bonding with water. The monolayer water contents ( $m_m$ , g/100 g of SNF) were slightly different, which were 4.96, 5.51, 5.30, and 5.57 g/100 g of SNF for lactose–MPI–OO, lactose–SPI–OO, trehalose–MPI–OO, and trehalose–SPI–OO systems, respectively, but similar corresponding  $a_w$  values (0.21–0.23) were obtained for all systems.

**Table 1.** Water Content (Mean Values  $\pm$  SD) in Freeze-Dried Carbohydrate–Protein–Oil (3:1:2) Systems after Equilibration at Various Water Activities ( $a_w$ ) for 5 Days at Room Temperature ( $24 \pm 1$  °C)

| system           | water content (g/100 g of SNF) |                 |                 |                 |                  |                  |                  |                  |
|------------------|--------------------------------|-----------------|-----------------|-----------------|------------------|------------------|------------------|------------------|
|                  | 0.00 $a_w$                     | 0.11 $a_w$      | 0.23 $a_w$      | 0.33 $a_w$      | 0.44 $a_w$       | 0.54 $a_w$       | 0.65 $a_w$       | 0.76 $a_w$       |
| lactose–MPI–OO   | 0.00 $\pm$ 0.00                | 3.44 $\pm$ 0.03 | 5.45 $\pm$ 0.02 | 7.00 $\pm$ 0.01 | 9.61 $\pm$ 0.03  | 12.62 $\pm$ 0.04 | 5.58 $\pm$ 0.06  | 8.21 $\pm$ 0.04  |
| lactose–SPI–OO   | 0.00 $\pm$ 0.00                | 3.29 $\pm$ 0.04 | 5.39 $\pm$ 0.01 | 6.85 $\pm$ 0.02 | 9.18 $\pm$ 0.02  | 11.90 $\pm$ 0.08 | 5.39 $\pm$ 0.09  | 7.78 $\pm$ 0.05  |
| trehalose–MPI–OO | 0.00 $\pm$ 0.00                | 3.66 $\pm$ 0.02 | 5.82 $\pm$ 0.07 | 7.48 $\pm$ 0.04 | 10.28 $\pm$ 0.04 | 14.27 $\pm$ 0.06 | 12.61 $\pm$ 0.02 | 14.23 $\pm$ 0.11 |
| trehalose–SPI–OO | 0.00 $\pm$ 0.00                | 3.57 $\pm$ 0.03 | 5.76 $\pm$ 0.02 | 7.34 $\pm$ 0.07 | 9.93 $\pm$ 0.01  | 13.78 $\pm$ 0.03 | 12.08 $\pm$ 0.03 | 13.07 $\pm$ 0.02 |

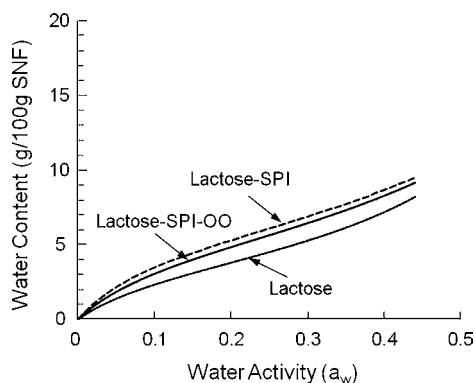


**Figure 2.** Water sorption isotherms of freeze-dried lactose,<sup>19</sup> lactose–SPI (3:1),<sup>19</sup> and lactose–SPI–OO (3:1:2) systems. The isotherms were modeled using the GAB relationship with experimental data.

**Glass Transition and Instant Sugar Crystallization.** The glass transition and sugar crystallization for anhydrous and humidified lactose–MPI–OO, lactose–SPI–OO, trehalose–MPI–OO, and trehalose–SPI–OO systems were measured, and the glass transition temperatures and instant sugar crystallization temperatures were read from the DSC thermographs. The second heating scans of DSC thermographs for lactose–SPI–OO and trehalose–SPI–OO systems at 0.33  $a_w$  are given in Figure 3 as examples, in which oil melting occurred

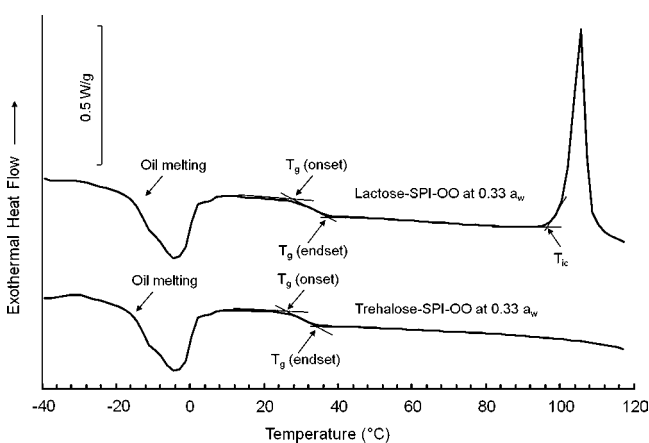


**Figure 3.** DSC thermographs of lactose–SPI–OO and trehalose–SPI–OO at 0.33  $a_w$ , showing oil melting, glass transition, and sugar crystallization. The thermographs were taken from the second heating scans (heating rate at 5 °C/min).

and was followed by a step endothermal change for glass transition. An exothermic peak, representing sugar crystallization, was observed only for lactose-containing systems at  $a_w$  above 0. The  $T_g$  of all systems, as shown in Table 2, was depressed as a result of water plasticization.<sup>11,28</sup> The  $T_g$  values of anhydrous lactose–MPI–OO and lactose–SPI–OO were similar to that of pure lactose. The  $T_g$  values of anhydrous trehalose–MPI–OO and trehalose–SPI–OO were slightly higher than that of pure trehalose, suggesting a possible better compatibility of trehalose with proteins, which may also contribute to the excellent protecting effects of trehalose on protein structures.<sup>34</sup> Proteins may affect the  $T_g$  of anhydrous systems by hydrogen bonding to sugar molecules, depending upon the type of proteins and sugars and the amount of proteins in the sugar–protein phase after emulsification, and

self-assembly of proteins at the oil droplet interfaces. The hydrogen bonding between sugars and proteins may be diminished in the presence of water. The plasticizing effect of water was dominant at increasing  $a_w$ , and in humidified systems, the  $T_g$  values were dependent upon the  $a_w$  and the component sugar (Figure 4B) rather than the water content (Figure 4A), regardless of the presence of protein and oil. As shown in Figure 4, it should be noted that the glass transition occurred only in the miscible nonfat solids components and the  $T_g$  values at varying  $a_w$  followed closely those of the component sugars.<sup>19</sup> This confirmed that the protein and carbohydrate components were largely phase-separated, and the  $T_g$  values corresponded to those of carbohydrates at most  $a_w$ ; i.e., the presence of protein affected the quantity of sorbed water, but the  $T_g$  corresponded to that of the carbohydrate at any constant  $a_w > 0$ .

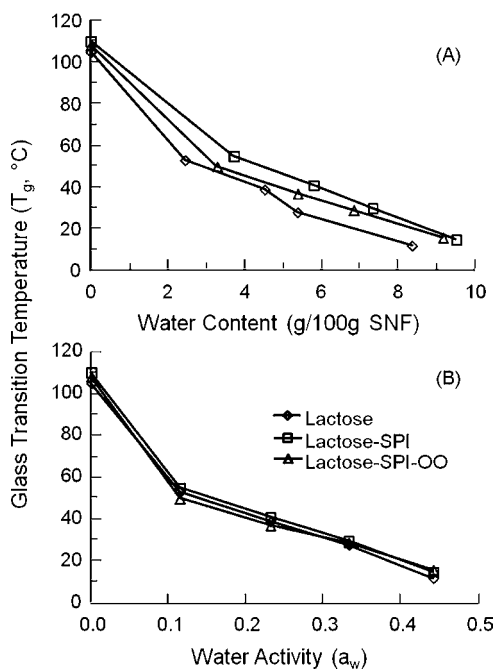
The instant crystallization at  $T_{ic}$ , showing rapid amorphous lactose crystallization, occurred in lactose–MPI–OO and lactose–SPI–OO systems at 0.11–0.44  $a_w$  (Table 3), but no  $T_{ic}$  was found for anhydrous systems. Our earlier studies reported that lactose alone crystallized at 174 °C at 0  $a_w$ , but no  $T_{ic}$  was observed for anhydrous systems in the presence of other components, e.g., protein<sup>19</sup> and hydrophilic vitamins.<sup>35</sup> These inhibiting effects of proteins and vitamins on sugar crystallization result from numerous factors, including restricted diffusion and retarded arrangements of sugar molecules to nucleate and form crystals. The  $T_{ic}$  decreased with increasing  $a_w$  as a result of water plasticization and confirmed phase separation of the sugar components. No instant crystallization of trehalose was found in trehalose–protein–oil systems (Figure 3), probably because an insufficient amount of water for trehalose to form dihydrate crystals was present and the interactions between trehalose and other components inhibited trehalose molecules to crystallize.<sup>19</sup>

**Oil Droplet Size Distribution.** The oil droplet size distributions for the emulsified systems are given in Figure 5. The volume weight mean diameter,  $D[4, 3]$ , and the median diameter,  $D[v, 0.5]$ , of emulsions are given in Table 4. The fresh lactose–MPI–OO and trehalose–MPI–OO emulsions showed monomodal distribution of droplets (curve a in panels A and C of Figure 5, respectively), while tail distribution was found in lactose–SPI–OO and trehalose–SPI–OO systems (curve a in panels B and D of Figure 5, respectively). During freezing, the oil droplets were immobilized and encapsulated in the maximally freeze-concentrated solutes. Freezing at –35 °C for 24 h and thawing at room temperature did not cause significant changes of the  $D[4, 3]$  and the oil droplet distributions (data not shown) in all systems, except in the trehalose–SPI–OO system, which showed an increase of  $D[4, 3]$  but similar  $D[v, 0.5]$ , indicating the increase of tail distribution (Table 4). The structure of freeze-dried materials was determined by (i) the oil droplet size distribution (size and number) during homogenization and (ii) the ice crystals (size and number) formed during freezing. After the sublimation of ice crystals, pores were left and a porous structure was obtained. Because of the low molecular mobility in the glassy matrices, the oil droplet size distribution was retained in the freeze-dried materials. Freeze-dried lactose–MPI–OO and trehalose–MPI–OO systems showed bimodal distribution (curve b in panels A and C of Figure 5, respectively), and freeze-dried lactose–SPI–OO and trehalose–SPI–OO showed increased tail distribution (curve b in panels B and D of Figure 5, respectively), of oil droplets, which could be a result of the

**Table 2. Onset and Endset Temperatures of Glass Transition ( $T_g$ , °C) at Various Water Activities ( $a_w$ ) for Freeze-Dried Lactose–MPI–OO (3:1:2), Lactose–SPI–OO (3:1:2), Trehalose–MPI–OO (3:1:2), and Trehalose–SPI–OO (3:1:2) Systems**

| system           |        | $T_g^a$ (°C) |              |              |              |              |
|------------------|--------|--------------|--------------|--------------|--------------|--------------|
|                  |        | 0.00 $a_w^b$ | 0.11 $a_w^c$ | 0.23 $a_w^d$ | 0.33 $a_w^e$ | 0.44 $a_w^f$ |
| lactose–MPI–OO   | onset  | 101          | 52           | 35           | 27           | 15           |
|                  | endset | 111          | 60           | 44           | 34           | 24           |
| lactose–SPI–OO   | onset  | 106          | 50           | 37           | 29           | 16           |
|                  | endset | 118          | 59           | 45           | 37           | 25           |
| trehalose–MPI–OO | onset  | 111          | 53           | 33           | 25           | 14           |
|                  | endset | 119          | 60           | 42           | 33           | 21           |
| trehalose–SPI–OO | onset  | 116          | 49           | 38           | 28           | 15           |
|                  | endset | 124          | 58           | 47           | 35           | 23           |

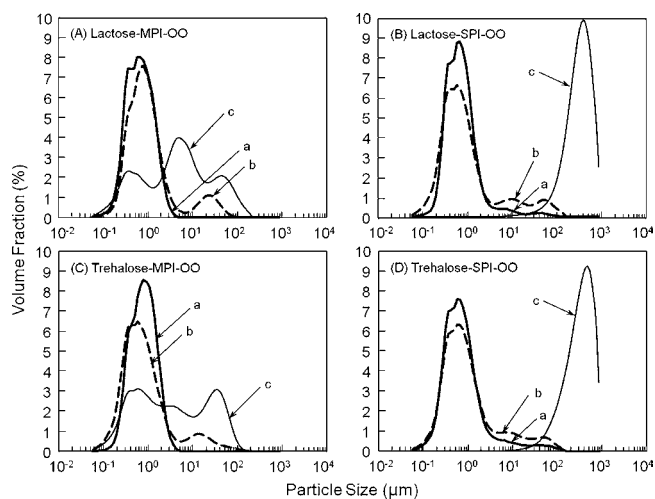
<sup>a</sup> $T_g \pm 1^\circ\text{C}$ . <sup>b</sup>DSC method: (i) from 25 to 150 °C at 5 °C/min, (ii) from 150 to –50 °C at 10 °C/min, and (iii) from –50 to 200 °C at 5 °C/min. <sup>c</sup>DSC method: (i) from 25 to 90 °C at 5 °C/min, (ii) from 90 to –50 °C at 10 °C/min, and (iii) from –50 to 150 °C at 5 °C/min. <sup>d</sup>DSC method: (i) from 10 to 70 °C at 5 °C/min, (ii) from 70 to –50 °C at 10 °C/min, and (iii) from –50 to 140 °C at 5 °C/min. <sup>e</sup>DSC method: (i) from 0 to 60 °C at 5 °C/min, (ii) from 60 to –50 °C at 10 °C/min, and (iii) from –50 to 130 °C at 5 °C/min. <sup>f</sup>DSC method: (i) from –10 to 50 °C at 5 °C/min, (ii) from 50 to –50 °C at 10 °C/min, and (iii) from –50 to 120 °C at 5 °C/min.

**Figure 4.** Effects of (A) water content (g/100 g of SNF) and (B) water activity ( $a_w$ ) on the onset temperature of glass transition ( $T_g$ , °C) in freeze-dried lactose,<sup>19</sup> lactose–SPI (3:1),<sup>19</sup> and lactose–SPI–OO (3:1:2) systems.**Table 3. Onset Temperature of Crystallization ( $T_{ic}$ , °C) in Freeze-Dried Lactose–MPI–OO (3:1:2) and Lactose–SPI–OO (3:1:2) Systems**

| system         | $T_{ic}^a$ (°C)  |            |            |            |            |
|----------------|------------------|------------|------------|------------|------------|
|                | 0.00 $a_w$       | 0.11 $a_w$ | 0.23 $a_w$ | 0.33 $a_w$ | 0.44 $a_w$ |
| lactose–MPI–OO | N/O <sup>b</sup> | 124        | 108        | 91         | 83         |
| lactose–SPI–OO | N/O <sup>b</sup> | 124        | 107        | 94         | 75         |

<sup>a</sup> $T_{ic} \pm 1^\circ\text{C}$ . <sup>b</sup>N/O = not observed.

breakdown of the thin interface during reconstitution. After storage at 0.76  $a_w$  for 5 days, a dramatic change of droplet size distribution was observed, corresponding to the crystallization of component sugar, which caused a complete rupture of the interfaces between the continuous and dispersed phases. Oil

**Figure 5.** Emulsion droplet size distribution of (A) lactose–MPI–OO (3:1:2), (B) lactose–SPI–OO (3:1:2), (C) trehalose–MPI–OO (3:1:2), and (D) trehalose–SPI–OO (3:1:2) systems. The emulsion samples for each system were (a) fresh emulsions that were measured within 1 h after homogenization, (b) freeze-dried materials that were reconstituted and measured, and (c) freeze-dried materials that were stored at 0.76  $a_w$  for 5 days, reconstituted and measured.

droplets were excluded from the encapsulants, and coalescence occurred.

**Stability of  $\alpha$ -Tocopherol as Affected by Water Activity.** The retention of  $\alpha$ -tocopherol in the freeze-dried materials was measured right after freeze-drying, which were  $94.8 \pm 0.8\%$ ,  $93.9 \pm 1.5\%$ ,  $95.1 \pm 1.6\%$ , and  $92.4 \pm 1.2\%$  for lactose–MPI–OO, lactose–SPI–OO, trehalose–MPI–OO, and trehalose–SPI–OO systems, respectively. These amounts of retained  $\alpha$ -tocopherol were taken as 100% for the storage study.

During 40 days of storage at 60 °C, rapid loss of  $\alpha$ -tocopherol occurred in all anhydrous systems within 3 days of storage, followed by less rapid loss up to 25 days of storage. From 25 to 40 days, constant retention of  $\alpha$ -tocopherol was found, except for the lactose–SPI–OO system, in which the  $\alpha$ -tocopherol content decreased but at a lower rate (Figure 6). After 40 days of storage, lactose–MPI–OO and trehalose–MPI–OO systems retained  $84.6 \pm 1.5\%$  and  $82.8 \pm 1.2\%$  of  $\alpha$ -

**Table 4. Volume Weight Mean Diameter,  $D[4, 3]$  (Mean  $\pm$  SD,  $\mu\text{m}$ ) and 50% Volume Percentile of Droplet Size Distribution,  $D[v, 0.5]$  (Median Mean Diameter  $\pm$  SD,  $\mu\text{m}$ ) of Lactose–MPI–OO (3:1:2), Lactose–SPI–OO (3:1:2), Trehalose–MPI–OO (3:1:2), and Trehalose–SPI–OO (3:1:2) Systems**

| system           | fresh emulsions <sup>a</sup> |                               | thawed emulsions <sup>b</sup> |                               | freeze-dried emulsions <sup>c</sup> |                               |
|------------------|------------------------------|-------------------------------|-------------------------------|-------------------------------|-------------------------------------|-------------------------------|
|                  | $D[4, 3]$ ( $\mu\text{m}$ )  | $D[v, 0.5]$ ( $\mu\text{m}$ ) | $D[4, 3]$ ( $\mu\text{m}$ )   | $D[v, 0.5]$ ( $\mu\text{m}$ ) | $D[4, 3]$ ( $\mu\text{m}$ )         | $D[v, 0.5]$ ( $\mu\text{m}$ ) |
| lactose–MPI–OO   | 0.75 $\pm$ 0.00              | 0.60 $\pm$ 0.00               | 0.88 $\pm$ 0.10               | 0.72 $\pm$ 0.01               | 3.26 $\pm$ 0.63                     | 0.77 $\pm$ 0.01               |
| lactose–SPI–OO   | 1.82 $\pm$ 0.03              | 0.59 $\pm$ 0.02               | 1.95 $\pm$ 0.20               | 0.62 $\pm$ 0.01               | 5.35 $\pm$ 0.15                     | 0.62 $\pm$ 0.01               |
| trehalose–MPI–OO | 0.85 $\pm$ 0.02              | 0.61 $\pm$ 0.02               | 1.03 $\pm$ 0.43               | 0.61 $\pm$ 0.01               | 3.03 $\pm$ 0.33                     | 0.62 $\pm$ 0.01               |
| trehalose–SPI–OO | 2.53 $\pm$ 0.16              | 0.60 $\pm$ 0.02               | 3.92 $\pm$ 0.70               | 0.63 $\pm$ 0.01               | 5.47 $\pm$ 1.27                     | 0.67 $\pm$ 0.02               |

<sup>a</sup>Measurements were carried out within 1 h after homogenization (fresh emulsions). <sup>b</sup>Measurements were carried out after thawing of frozen emulsions. Fresh emulsions were frozen at  $-35$  °C for 24 h and then thawed at room temperature for 1 h. <sup>c</sup>Measurements were carried out after reconstitution of freeze-dried materials.

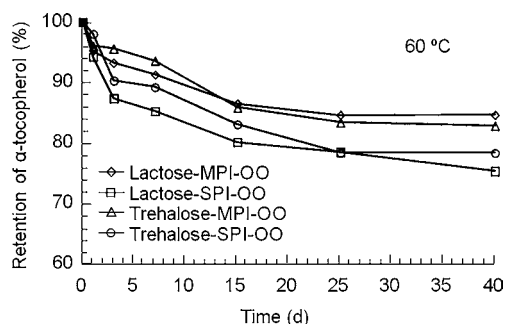


**Figure 6.** Retention (%) of  $\alpha$ -tocopherol in anhydrous freeze-dried lactose–MPI–OO (3:1:2), lactose–SPI–OO (3:1:2), trehalose–MPI–OO (3:1:2), and trehalose–SPI–OO (3:1:2) systems during 40 days of storage at 60 °C.

tocopherol, respectively, while lactose–SPI–OO and trehalose–SPI–OO systems retained smaller amounts of  $\alpha$ -tocopherol, which were  $75.3 \pm 2.1\%$  and  $78.3 \pm 1.7\%$ , respectively.

The retention of  $\alpha$ -tocopherol after 5 days of storage at various  $a_w$  conditions and the water content of systems at corresponding  $a_w$  were plotted as a function of  $a_w$  (Figure 7).  $\alpha$ -Tocopherol was the most stable at 0  $a_w$ . MPI-stabilized systems showed higher retention. This high retention of  $\alpha$ -tocopherol confirmed our hypothesis that  $\alpha$ -tocopherol did not show good

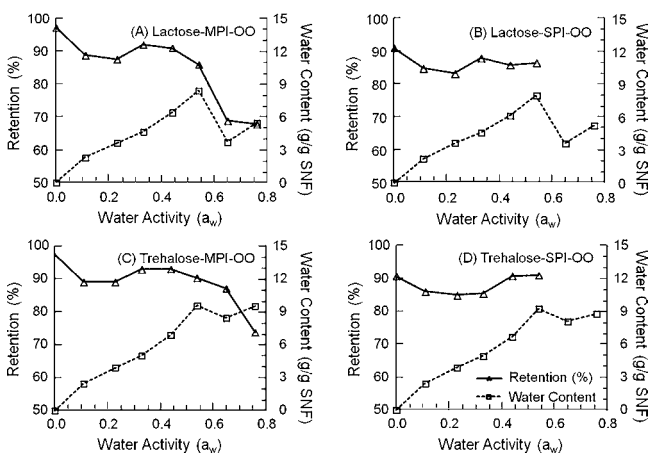


**Figure 7.** Retention (%) of  $\alpha$ -tocopherol and water content (g/100 g of SNF) for freeze-dried (A) lactose–MPI–OO (3:1:2), (B) lactose–SPI–OO (3:1:2), (C) trehalose–MPI–OO (3:1:2), and (D) trehalose–SPI–OO (3:1:2) systems after storage at various  $a_w$  (0.0–0.76) for 5 days.

antioxidant activity in anhydrous systems, which could be similar to bulk oil systems, and the stability of  $\alpha$ -tocopherol was assured by its immobilization in the glassy solid matrices.  $\alpha$ -Tocopherol is a hydrophobic compound but contains a hydrophilic OH group, which is surface-active to be oriented in the oil–water interface to protect oil against oxidation.<sup>23</sup> During freezing, water molecules formed ice crystals and the glassy solids with  $\alpha$ -tocopherol at interfaces were formed. Freeze-drying removed ice crystals by sublimation and retained the structures formed during freezing, explaining a relatively high stability of  $\alpha$ -tocopherol at low  $a_w$ .

$\alpha$ -Tocopherol showed highest stability at 0  $a_w$  in all of the systems. A minimum retention of  $\alpha$ -tocopherol was found at 0.11–0.23  $a_w$  (at 0.11–0.33  $a_w$  for the trehalose–SPI–OO system), which agreed with rapid lipid oxidation at low  $a_w$ .<sup>7</sup> At increasing  $a_w$  (0.33–0.44  $a_w$  for the trehalose–SPI–OO system and from 0.23 to 0.33  $a_w$  for all other systems), the retention of  $\alpha$ -tocopherol increased, showing that the loss of hydrophobic  $\alpha$ -tocopherol coincided with the oxidation of the oil.<sup>6–8</sup> At higher than 0.54  $a_w$ , the loss of  $\alpha$ -tocopherol was concomitant to component sugar crystallization. The reasons for the loss of  $\alpha$ -tocopherol could be (i) exclusion of oil droplets from the matrices causing a loss of protection, (ii) increased availability of oxygen from the environment, and (iii) increased mobilization of  $\alpha$ -tocopherol at the interfaces and its consumption as an antioxidant. Some differences in  $\alpha$ -tocopherol stability at crystallizing conditions may also relate to higher solubility of trehalose and retention of a protective trehalose “syrup” on entrapped oil particles. SPI-containing systems at  $a_w > 0.54$  showed a difficulty in reconstitution of freeze-dried materials and, therefore, a difficulty in the extraction of  $\alpha$ -tocopherol, possibly because of the gelation of SPI with a sufficient amount of water, which was released from sugar crystallization. Extraction of oil from such systems, however, was technically difficult, and data at higher  $a_w$  values were not included.

Materials equilibrated at various  $a_w$  (referring to  $a_w$  at room temperature) were transferred to 60 °C and kept for 10 days. At 60 °C, systems with  $T_g$  above (0  $a_w$ ) and around (0.11  $a_w$ ) the storage temperature retained  $\alpha$ -tocopherol in the glassy structures, indicating that the glassy state protected  $\alpha$ -tocopherol. The loss of  $\alpha$ -tocopherol occurred at 0.23  $a_w$  and above, at which the heat-induced plasticization depressed the  $T_g$  of the systems to below the storage temperature, followed by component sugar crystallization (Figure 8). Lactose crystallization had a more severe effect on the loss of  $\alpha$ -tocopherol compared to trehalose crystallization. Trehalose crystallized to a lesser extent as a dihydrate and retained a higher amount of water in the crystals. The higher solubility of trehalose

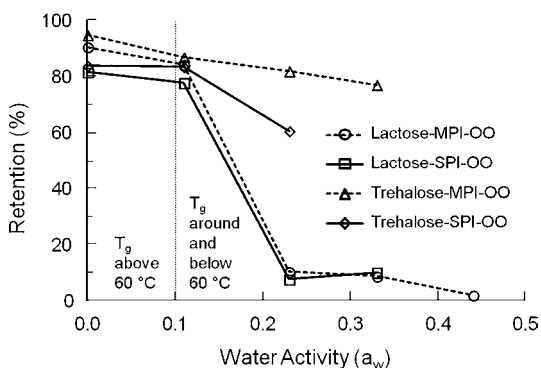


**Figure 8.** Retention (%) of  $\alpha$ -tocopherol for freeze-dried lactose–MPI–OO (3:1:2), lactose–SPI–OO (3:1:2), trehalose–MPI–OO (3:1:2), and trehalose–SPI–OO (3:1:2) systems after storage at 60 °C for 10 days. The materials were equilibrated to various  $a_w$  (0.0–0.44) for 5 days before transportation to 60 °C.

dihydrate also allowed trehalose to dissolve in water and form trehalose syrup, which possibly protected the sensitive compounds.<sup>19</sup> The rapid loss of  $\alpha$ -tocopherol at sugar crystallization further suggested that a relatively large quantity of  $\alpha$ -tocopherol could be located at the oil–water interface.

Significant color changes (browning) were visually observed at  $a_w \geq 0.23$  after storage at 60 °C for lactose-containing systems. Slight color changes were found in trehalose-containing systems at  $a_w \geq 0.65$  after storage at 60 °C, which could be due to the presence of traces of reducing sugars in proteins. SPI-containing systems at  $a_w > 0.33$  in storage at 60 °C showed a difficulty in reconstitution of freeze-dried materials, which was due to the possible gelation of SPI at these conditions.

#### Matrix Structure and Stability of $\alpha$ -Tocopherol.

Schematic diagrams of the structure formation during processing and structural changes during storage for model systems are shown in Figure 9. Homogenization broke down the oil phase into small droplets and stabilized the dispersed phase in the water phase by the amphiphilic proteins<sup>36</sup> (panels

A and B of Figure 9). During freezing, ice crystals were formed and the solutes (sugar–protein) were freeze-concentrated. The oil droplets were immobilized and encapsulated in the continuous unfrozen solute phase (Figure 9C). Pores were left after the sublimation of ice crystals, and the size of ice crystals formed during freezing determined the porosity of the freeze-dried materials. The oil droplets were encapsulated in the matrices, although partial exposure to the pores was possible (Figure 9D). During storage at various  $a_w$  conditions, water was sorbed by the amorphous solutes because of the high hygroscopy and porosity of the freeze-dried materials (Figure 9E). Labuza<sup>7</sup> has found that at 0 and low  $a_w$ , lipid oxidation occurred rapidly. At increasing  $a_w$ , water exerted a protective effect, which attributed to the hydration of metal catalysts decreasing their effectiveness and hydrogen bonding to peroxides. This explained the low retention of hydrophobic  $\alpha$ -tocopherol at low  $a_w$ .  $\alpha$ -Tocopherol could be consumed as an antioxidant and showed lower retention, accounting for the decreased oxidation of the solvent lipid. In our study, the stability of  $\alpha$ -tocopherol at 0  $a_w$  was possibly enhanced by partial immobilization at interfaces of the oil and the glassy matrices that could reduce the antioxidant activity of  $\alpha$ -tocopherol, i.e., corresponding to lower consumption as an antioxidant, at 0  $a_w$ . At water activities that depressed the  $T_g$  to below the storage temperatures (room temperature or 60 °C) and allowed the component sugar to crystallize time-dependently, the stability of  $\alpha$ -tocopherol was no longer retained because of the increased exposure of lipids to the surrounding atmosphere. Structural changes, e.g., collapse (Figure 9F) and sugar crystallization (Figure 9G), caused the exclusion of the oil droplets from the encapsulants to the environment and coalescence of the oil droplets, leading to losses of  $\alpha$ -tocopherol.<sup>35</sup>

In conclusion, this study showed that stability of  $\alpha$ -tocopherol in freeze-dried carbohydrate–protein–oil emulsions was affected by water plasticization and physical changes. This information contributes to the use of carbohydrate–protein systems as structure-forming matrices for stabilization of

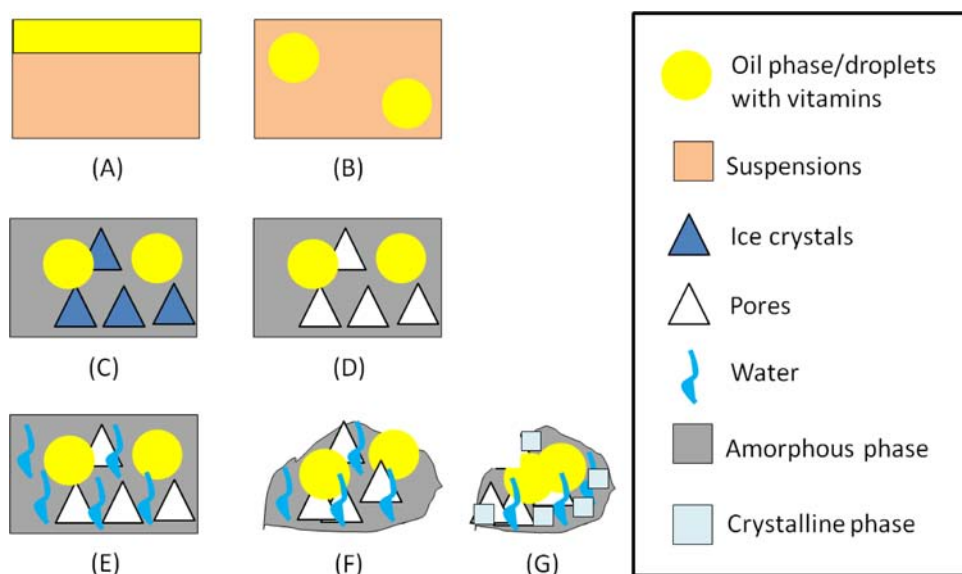


**Figure 9.** Diagrams of the model systems (A) before and (B) after homogenization, (C) frozen, and (D) freeze-dried. During storage, (E) water-plasticization and (F) collapse occurred because of water sorption. (G) Crystallization of sugars may lead to exclusion and coalescence of the oil droplets. The symbols do not represent the real size of components.

hydrophobic nutrients. Freezing and freeze-drying of emulsions encapsulated oil droplets in structure-forming sugar–protein matrices. Milk proteins and soy proteins showed good emulsifying properties as well as contribution to the matrix properties. The structure of the systems was well-retained during processing, although changes of oil droplet size distribution occurred because of the ruptures of the interfaces on reconstitution. The presence of oil slightly altered the water sorption behavior of the matrices but reduced the crystallization rate of the component sugars at high water activity conditions.  $\alpha$ -Tocopherol was probably immobilized at anhydrous conditions at interfaces and did not show antioxidant activity, and the stability of  $\alpha$ -tocopherol was retained in anhydrous freeze-dried sugar–protein matrices. Water activity affected the stability of  $\alpha$ -tocopherol by affecting the rate of lipid oxidation and the antioxidant activity of  $\alpha$ -tocopherol. Water-sorption- and thermal-induced crystallization of the component sugars caused dramatic structural changes of the matrices, which were believed to be the main cause of the loss of the stability of  $\alpha$ -tocopherol. Dependent upon the properties (type of crystals and their solubility) of the component sugars, the effects of sugar crystallization differed. Because sugar crystallization is a time-dependent phenomenon above the  $T_g$  of the matrices, more studies are required to understand the changes above  $T_g$  of the systems and the effects of structural changes on the stability of encapsulated particles.

## AUTHOR INFORMATION

### Corresponding Author

\*Telephone: +353214902386. Fax: +353214276398. E-mail: yrjo.roos@ucc.ie.

### Funding

This study was supported by the Department of Agriculture, Food and the Marine, Ireland, Food Institutional Research Measure (FIRM) Project 08RDC695.

### Notes

The authors declare no competing financial interest.

## ABBREVIATIONS USED

$a_w$ , water activity; MPI, milk protein isolate; SPI, soy protein isolate; OO, olive oil; w/w, weight per weight;  $T_g'$ , glass transition temperature of the maximally freeze-concentrated solutes;  $T_m'$ , ice-melting temperature in the maximally freeze-concentrated systems; SNF, solid nonfat; GAB, Guggenheim–Anderson–de Boer relationship;  $m_m$ , monolayer water content;  $T_g$ , glass transition temperature;  $T_{ic}$ , instant crystallization temperature; w/v, weight per volume

## REFERENCES

- Zingg, J.-M.; Azzi, A. Non-antioxidant activities of vitamin E. *Curr. Med. Chem.* **2004**, *11* (9), 1113–1133.
- Lea, C. H.; Ward, R. J. Relative activities of the seven tocopherols. *J. Sci. Food Agric.* **1959**, *10*, 537–548.
- Riejtens, I. M. C. M.; Boersma, M. G.; de Haan, L.; Spenkelink, B.; Awad, H. M.; Cnubben, N. H. P.; van Zanden, J. J.; van der Woude, H.; Alink, G. M.; Koeman, J. H. The pro-oxidant chemistry of the natural antioxidants vitamin C, vitamin E, carotenoids and flavonoids. *Environ. Toxicol. Pharmacol.* **2002**, *11*, 321–333.
- Valenzuela, A.; Sanhueza, J.; Nieto, S. Differential inhibitory effect of  $\alpha$ -,  $\beta$ -,  $\gamma$ -, and  $\delta$ -tocopherols on the metal-induced oxidation of cholesterol in unilamellar phospholipid–cholesterol liposomes. *J. Food Sci.* **2002**, *67* (6), 2051–2055.

- Kanner, J.; Hartel, S.; Mendel, H. Content and stability of  $\alpha$ -tocopherol in fresh and dehydrated pepper fruits (*Capsicum annuum* L.). *J. Agric. Food Chem.* **1979**, *27* (6), 1316–1318.
- Widicus, W. A.; Kirk, J. R.; Gregory, J. F. Storage stability of  $\alpha$ -tocopherol in a dehydrated model food system containing no fat. *J. Food Sci.* **1980**, *45*, 1015–1018.
- Labuza, T. P. The effect of water activity on reaction kinetics in food deterioration. *Food Technol.* **1980**, *34* (4), 36–41.
- Widicus, W. A.; Kirk, J. R. Storage stability of  $\alpha$ -tocopherol in a dehydrated model food system containing methyl linoleate. *J. Food Sci.* **1981**, *46*, 813–816.
- Kamal-Eldin, A.; Mäkinen, M.; Lampi, A.-M.; Hopia, A. A multivariate study of  $\alpha$ -tocopherol and hydroperoxide interaction during the oxidation of methyl linoleate. *Eur. Food Res. Technol.* **2002**, *214*, 52–57.
- Roos, Y. H. *Phase Transitions in Food*; Academic Press: San Diego, CA, 1995.
- Slade, L.; Levine, H. Beyond water activity: Recent advances based on an alternative approach to the assessment of food quality and safety. *Crit. Rev. Food Sci. Nutr.* **1991**, *30* (2–3), 115–360.
- Kaushik, V.; Roos, Y. H. Lipid encapsulation in glassy matrices of sugar–gelatin systems in freeze-drying. *Int. J. Food Prop.* **2008**, *11*, 363–378.
- Flink, J. M. Retention of 2-propanol at low concentration by freeze-drying carbohydrate solutions. *J. Food Sci.* **1972**, *37*, 617–618.
- Roos, Y.; Karel, M. Phase transitions of mixtures of amorphous polysaccharides and sugars. *Biotechnol. Prog.* **1991**, *7* (1), 49–53.
- Goubet, I.; Le Quere, J. L.; Voilley, A. J. Retention of aroma compounds by carbohydrates: Influence of their physicochemical characteristics and of their physical state. A review. *J. Agric. Food Chem.* **1998**, *46*, 1981–1990.
- Grattard, N.; Salaün, F.; Champion, D.; Roudaut, G.; Le Meste, M. Influence of physical state and molecular mobility of freeze-dried maltodextrin matrices of the oxidation rate of encapsulated lipids. *J. Food Sci.* **2002**, *67* (8), 3002–3010.
- Farias, M. C.; Moura, M. L.; Andrade, L.; Leão, M. H. M. R. Encapsulation of the  $\alpha$ -tocopherol in a glassy food model matrix. *Mater. Res.* **2007**, *10* (1), 57–62.
- Roudaut, G.; Simatos, D.; Champion, D.; Contreras-Lopez, E.; Le Meste, M. Molecular mobility around the glass transition temperature: A mini review. *Innovative Food Sci. Emerging Technol.* **2004**, *5*, 127–134.
- Zhou, Y.; Roos, Y. H. Characterization of carbohydrate–protein matrices for nutrient delivery. *J. Food Sci.* **2011**, *76* (4), E368–376.
- McClements, D. J.; Decker, E. A.; Weiss, J. Emulsion-based delivery systems for lipophilic bioactive components. *J. Food Sci.* **2007**, *72* (8), 109–124.
- Labuza, T. P.; McNally, L.; Gallagher, D.; Hawkes, J.; Hurtado, F. Stability of intermediate moisture foods. 1. Lipid oxidation. *J. Food Sci.* **1972**, *37*, 154–159.
- Porter, W. L.; Black, E. D.; Drolet, A. M. Use of polyamide oxidative fluorescence test on lipid emulsions: Contrast in relative effectiveness of antioxidants in bulk versus dispersed systems. *J. Agric. Food Chem.* **1989**, *37*, 615–624.
- Frankel, E. N.; Huang, S.-W.; Kanner, J.; German, J. B. Interfacial phenomena in the evaluation of antioxidants: Bulk oils vs emulsions. *J. Agric. Food Chem.* **1994**, *42*, 1054–1059.
- Contreras-Guzmán, E.; Strong, F. C., III Determination of total tocopherols in grains, grain products, and commercial oils, with only slight saponification, and by a new reaction with cupric ion. *J. Agric. Food Chem.* **1982**, *30*, 1109–1112.
- Labuza, T. P.; Kaananer, A.; Chen, J. Y. Effect of temperature on the moisture sorption isotherms and water activity shift of two dehydrate foods. *J. Food Sci.* **1985**, *50*, 385–391.
- Berlin, E.; Anderson, B. A.; Pallansch, M. J. Water vapor sorption properties of various dried milks and wheys. *J. Dairy Sci.* **1968**, *51* (9), 1339–1344.
- Roos, Y. H. Water activity and physical state effects on amorphous food stability. *J. Food Process. Preserv.* **1993**, *16*, 433–447.



- (28) Roos, Y.; Karel, M. Differential scanning calorimetry study of phase transitions affecting the quality of dehydrated materials. *Biotechnol. Prog.* **1990**, *6* (2), 159–63.
- (29) O'Regan, J.; Mulvihill, D. M. Sodium caseinate-maltodextrin conjugate stabilized double emulsions: Encapsulation and stability. *Food Res. Int.* **2010**, *43*, 224–231.
- (30) Cornacchia, L.; Roos, Y. H. Stability of  $\beta$ -carotene in protein-stabilized oil-in-water delivery systems. *J. Agric. Food Chem.* **2011**, *59*, 7013–7020.
- (31) Hewavitharana, A. K.; Van Brakel, A. S.; Harnett, M. Simultaneous liquid chromatographic determination of vitamins A, E and  $\beta$ -carotene in common dairy foods. *Int. Dairy J.* **1996**, *6*, 613–624.
- (32) Imamura, K.; Iwai, M.; Ogawa, T.; Sakiyama, T.; Nakanishi, K. Evaluation of hydration states of protein in freeze-dried amorphous sugar matrix. *J. Pharm. Sci.* **2001**, *90* (12), 1955–1963.
- (33) Silalai, N.; Roos, Y. H. Roles of water and solids composition in the control of glass transition and stickiness of milk powders. *J. Food Sci.* **2010**, *75*, E285–296.
- (34) López-Díez, E. C.; Bone, S. The interaction of trypsin with trehalose: An investigation of protein preservation mechanisms. *Biochim. Biophys. Acta* **2004**, *1673*, 139–148.
- (35) Zhou, Y.; Roos, Y. H. Stability and plasticizing and crystallization effects of vitamins in amorphous sugar systems. *J. Agric. Food Chem.* **2012**, *60*, 1075–1083.
- (36) McClements, D. J. Protein-stabilized emulsions. *Curr. Opin. Colloid Interface Sci.* **2004**, *9*, 305–313.